HHS Public Access

Author manuscript

J Cogn Neurosci. Author manuscript; available in PMC 2020 February 18.

Published in final edited form as:

J Cogn Neurosci. 2019 December ; 31(12): 1857–1872. doi:10.1162/jocn_a_01454.

Structural and Functional MRI Evidence for Distinct Medial Temporal and Prefrontal Roles in Context-dependent Relational Memory

Hillary Schwarb[1], **Curtis L. Johnson**[2], **Michael R. Dulas**[1], **Matthew D. J. McGarry**[3], **Joseph L. Holtrop**[4], **Patrick D. Watson**[5], **Jane X. Wang**[6], **Joel L. Voss**[7], **Bradley P. Sutton**[1], **Neal J. Cohen**[1]

[1]University of Illinois at Urbana-Champaign,

[2]University of Delaware,

[3]Dartmouth College,

[4]St. Jude Children's Research Hospital, Memphis, TN,

[5]Minerva Schools at Keck Graduate Institute, San Francisco, CA,

[6]DeepMind, London,

[7]Northwestern University, Feinberg School of Medicine

Abstract

Declarative memory is supported by distributed brain networks in which the medial-temporal lobes (MTLs) and pFC serve as important hubs. Identifying the unique and shared contributions of these regions to successful memory performance is an active area of research, and a growing literature suggests that these structures often work together to support declarative memory. Here, we present data from a context-dependent relational memory task in which participants learned that individuals belonged in a single room in each of two buildings. Room assignment was consistent with an underlying contextual rule structure in which male and female participants were assigned to opposite sides of a building and the side assignment switched between buildings. In two experiments, neural correlates of performance on this task were evaluated using multiple neuroimaging tools: diffusion tensor imaging (Experiment 1), magnetic resonance elastography (Experiment 1), and functional MRI (Experiment 2). Structural and functional data from each individual modality provided complementary and consistent evidence that the hippocampus and the adjacent white matter tract (i.e., fornix) supported relational memory, whereas the ventromedial pFC/OFC (vmPFC/OFC) and the white matter tract connecting vmPFC/OFC to MTL (i.e., uncinate fasciculus) supported memory-guided rule use. Together, these data suggest that MTL and pFC structures differentially contribute to and support contextually guided relational memory.

Reprint requests should be sent to Hillary Schwarb, University of Illinois at Urbana-Champaign, 405 N. Mathews Ave., M/C 251, Urbana, IL 61801-3028, or via schwarb2@illinois.edu.

INTRODUCTION

As we interact with the world, we are constantly encoding information, updating mental representations, and altering our behavior to meet changing situational demands; this is an essential part of the human experience integrally tied to memory (Moscovitch, Cabeza, Winocur, & Nadel, 2016; Cohen, 2015; Eichenbaum & Cohen, 2014; Maguire & Mullally, 2013). Such behaviors are often context dependent; for example, remembering that to visit your friend at work, you need to go to her third-floor office, but to visit her at home, you need to go to her first-floor apartment. Multiple lines of converging neuroscience research have implicated both the medial-temporal lobes (MTLs) and the pFC in various aspects and kinds of memory (e.g., Schwarb, Johnson, McGarry, & Cohen, 2016; Schlichting & Preston, 2015; Schwarb et al., 2015; Wang, Cohen, & Voss, 2015; Zeithamova, Dominick, & Preston, 2012; Zeithamova, Schlichting, & Preston, 2012; Battaglia, Benchenane, Sirota, Pennartz, & Wiener, 2011; Eichenbaum, Yonelinas, & Ranganath, 2007; Bunge, Burrows, & Wagner, 2004; Simons & Spiers, 2003). In recent years, understanding the unique and shared contributions of these distinct but interconnected regions has become an active and important area of research.

There is a vast literature highlighting the essential role that the MTL plays in episodic and relational/associative memory in both humans and animals (for reviews, see Voss, Bridge, Cohen, & Walker, 2017; Ranganath & Ritchey, 2012; Ranganath, 2010; Eichenbaum & Cohen, 2001; Cohen & Eichenbaum, 1993). Relational memory theory posits that the hippocampus, in particular, automatically and obligatorily binds information into coherent memory representations that can then be used flexibly in a variety of situations (Monti et al., 2015; Rubin, Watson, Duff, & Cohen, 2014; Konkel & Cohen, 2009; Ryan, Althoff, Whitlow, & Cohen, 2000; Cohen & Eichenbaum, 1993). This information includes associations among the elements of experiences and the specific spatial and temporal locations in which those elements occurred. Recent extensions of this theory (Rubin, Schwarb, Lucas, Dulas, & Cohen, 2017; Wang et al., 2015) have proposed a complementary role of the pFC, which is known to extract regularities among these specific memories and to abstract rules/schemas used to guide behavior and accomplish task goals (Badre & Nee, 2018; Gershman, Norman, & Niv, 2015; Kroes & Fernandez, 2012; Miller, Freedman, & Wallis, 2002; Miller & Cohen, 2001; Miller, 1999a, 1999b). As such, pFC is essential for strategic control over memory retrieval given a particular context (Badre & Nee, 2018; Wang et al., 2015; Preston & Eichenbaum, 2013; Buckner, 2003). Here, we refer to process as “memory-guided rule use,” highlighting both the nature of the acquired memory representations and their use in guiding a response.

There is an accumulating body of evidence highlighting the interactive role of pFC and MTL during mnemonic processing (e.g., Ritchey, Libby, & Ranganath, 2015; Ranganath & Ritchey, 2012; Zeithamova, Dominick, et al., 2012; Ranganath, 2010; Zeithamova & Preston, 2010; Ranganath, Heller, Cohen, Brozinsky, & Rissman, 2005; Bunge et al., 2004). These data demonstrate not only that are MTL and pFC structures functionally interconnected but also that their shared contributions are essential for successful memory performance. Furthermore, MTL and pFC structures are anatomically connected (Wendelken et al., 2015; Sasson, Doniger, Pasternak, Tarrasch, & Assaf, 2013; Von Der

Heide, Skipper, Klobusicky, & Olson, 2013) and are thus well suited to interactively contribute to memory (Preston & Eichenbaum, 2013). The integrity of these anatomical connections, ensuring more efficient communication, likely plays a critical role in successful memory performance. Indeed, to fully appreciate mnemonic behavior and the neural systems that support this behavior, a multidimensional, converging approach is essential.

The current work embraces this approach by combining multiple complementary neuroimaging tools—namely, diffusion tensor imaging (DTI), magnetic resonance elastography (MRE), and functional MRI (fMRI)—to explore both the structural and functional contributions of pFC and MTL to relational memory processing and memory-guided rule use. Additionally, although the neural correlates of relational memory and memory-guided rule use have been investigated independently, their unique and shared contributions to memory performance in a single task has yet to be explored. Exploring the engagement of these processes in a single task allows for a more direct comparison of behavioral outcomes and the neural mechanisms that support them. Therefore, in the current work, we present two experiments using a context-dependent relational memory task (Schwarb et al., 2015) designed to engage both the relational memory system and the memory-guided rule use system and also to dissociate the multiple sources of memory information that unfold over time and contribute to successful memory performance. In this task, participants learned face–room pairings in two different buildings such that room assignment was consistent with an underlying incidental contextual rule structure that could be used to guide behavior. We applied multiple and converging neuroimaging tools to explore structure–function relationships, supporting both relational memory and memory-guided rule use processes. We hypothesized that, across both experiments and all three imaging modalities, MTL structures would uniquely support participants' ability to remember specific face–room association (relational memory; Eichenbaum & Cohen, 2001; Cohen & Eichenbaum, 1993) whereas pFC (via its anatomical connection to the MTL) would uniquely support the ability to extract the conditional rule structure from the remembered associations and then use the rule to guide behavior (memory-guided control; Preston & Eichenbaum, 2013).

In Experiment 1, two complementary structural neuroimaging techniques were applied, DTI and MRE, to investigate the joint and separable contributions of MTL and pFC structures and their connections to relational memory and memory-guided rule use. Both DTI and MRE provide microstructural measures of tissue integrity. DTI tractography provides a structural measure of white matter tract integrity that allows us to investigate structural dissociations between MTL-specific fiber tracts (i.e., fimbria; Wendelken et al., 2015; Douet & Chang, 2014) and fiber tracts that connect MTL to pFC (i.e., uncinate fasciculus [UF]; Wendelken et al., 2015; Von Der Heide et al., 2013; Price et al., 2008). MRE is an emerging technology that provides a quantitative measure of the mechanical properties of tissue by assessing regional microstructural integrity (Hiscox, Johnson, McGarry, Perrins, et al., 2018; Johnson et al., 2016). Although DTI informs us about the structural integrity of white matter tracts, MRE provides measures of the microstructural integrity of the anatomical regions that those white matter tracts connect. MRE-derived measures of structural integrity in both the hippocampus and ventromedial pFC (vmPFC)/OFC (the terminating structure of the UF) were considered here. We predicted that both DTI-measured fimbria integrity and MRE-

measured hippocampal integrity would be related to successful relational memory, while DTI-measured UF integrity and MRE-measured vmPFC/OFC integrity would be related to successful memory-guided rule use. Volume, a measure of macrostructural tissue integrity that often relates to cognitive outcomes in older adults and patient populations, was also considered.

In Experiment 2, a second group of naive participants completed the same memory task as in Experiment 1, while undergoing an fMRI scan. This design afforded the opportunity to consider relational memory-specific neural correlates, distinct from the neural correlates that support memory-guided rule use, and to further probe the findings from Experiment 1 using a distinct functional neuroimaging tool that provides a complementary lens to address the questions of interest. Based on the results of Experiment 1, we predicted that relational memory retrieval processes would activate the hippocampus whereas memory-guided rule use processes would activate the vmPFC/OFC. Activity was assessed only at retrieval. fMRI also affords the unique opportunity to investigate the contributions of these regions at different stages of the experiment when different information is available to the participant rather than overall performance.

METHODS

Participants

In Experiment 1, 20 right-handed healthy young male volunteers (18–33 years old) participated in the study. Only male participants were included because of known sex differences in the mechanical properties of the brain (Arani et al., 2015; Sack et al., 2009). Each provided informed, written consent following study approval by our institutional review board and was treated in accordance to American Psychological Association (APA)-approved guidelines (APA, 1992). All volunteers underwent a single MRI scanning session followed by a behavioral testing session. Participations were compensated $15/hr. Hippocampal MRE data, in relation to performance on a spatial reconstruction task, both the word list and logical memory tests from the Weschler Memory Scale and the Stroop task from this sample, have been reported elsewhere (Schwarb et al., 2015).

In Experiment 2, 20 volunteers (ages 18–23 years, 12 women) recruited from the Northwestern University community participated in this study. All participants were right-handed, with normal or corrected-to-normal vision. Participants gave informed consent and were treated in accordance to APA-approved guidelines (APA, 1992). The Northwestern University Institutional Review Board approved all procedures. All volunteers underwent a single MRI scanning session. Participations were compensated $30/hr.

Behavioral Task

The basic task design has been described elsewhere (Schwarb et al., 2015; Experiment 2). Stimuli included two buildings, differing only in color (one purple, one blue), each with three floors and seven rooms per floor. Each building was sized to 29.5° × 16.9° of visual angle. There was a gradation in shading across the columns that radiated out from the center column for both the blue and purple buildings. The buildings were identical across blocks.

In Experiment 1, 32 male and 32 female full-color images were selected from our face database (see Althoff & Cohen, 1999). Each face was sized to 2.6° × 3.1° (“small”; used during the study phase and in the latter portion of the test phase) and 6.9° × 7.9° of visual angle (“large”; used in the initial portion of the test phase). Four male and four female faces were presented one at a time in each of four experimental blocks. Each face appeared in one room in each building. Male and female faces always appeared on opposite sides of each building, and this gender-by-side rule alternated between buildings (e.g., male faces appeared on the left in the blue building and on the right in the purple building, whereas female faces appeared on the right in the blue building and on the left in the purple building). Each face occupied a unique room during each experimental block.

Blocks were divided into a study phase and a test phase. During the study phase (Figure 1A), participants learned where each of the eight faces belonged in one building before learning where those same faces belonged in the other building. Each face was studied three times in each building. On every study trial, participants were asked which side of the building the face appeared on; this served as the encoding question, and participants responded with a button push indicating their selection. This encoding question drew the participants’ attention to the two sides of the building but importantly did not highlight the gender of each face. Each study trial lasted 3 sec, and trials were separated by a 250-msec intertrial interval. The test phase immediately followed the study phase of each block. During the test phase (Figure 1B), a “large” face was centrally presented for 3 sec (i.e., face-only period) before being replaced by an empty gray building (i.e., gray-building period). After 2.5 sec, one of the colored buildings appeared (i.e., color-building period). After an additional 2.5 sec, the “small” face reappeared in the center of the screen, and participants used the mouse to position the face in the room in which it was studied. Each of the eight studied faces was tested once, such that four faces were tested in the purple building and four were tested in the blue building; test order was random. Four unstudied novel faces (two male and two female) were also included at test to evaluate pure rule learning. Participants were instructed to “place any new face where you think it fits best.” Therefore, a rule-consistent response was conditional on considering both building context and gender information. There were four blocks.

Before the start of the experiment, participants were given task instructions and then completed 12 practice study trials and 12 practice test trials. All remaining questions about the procedure were answered at this time. All stimuli were presented on a 21-in. color monitor, and data were collected using Presentation software (Neurobehavioral Systems, www.neuro-bs.com) on a Windows-based computer.

In Experiment 2, the design was similar to that used in Experiment 1 with four modifications to make it fMRI compatible: (1) Participants completed eight experimental blocks each, including a study phase and a testing phase.(2) The testing phase was identical to Experiment 1 except that a variable ISI of either 2, 4, or 8 sec was included between the face-only and gray-building periods, as well as between the gray-building and color-building periods.(3) Each trial ended after the participant responded or 4.5 sec had passed. After 4.5 sec with no response, a red “X” replaced the face stimulus for 500 msec, indicating that the participant needed to respond more quickly. (4) Practice was performed inside a mock MRI

scanner immediately before scanning. The mock scanner recreated the physical enclosure, table, ambient sounds, head coil, and roller ball mouse of the MRI scanner. Discrete phases separated by jitter were included to investigate how memory processes unfold over time and to dissociate relational memory processes in the absence of rule-relevant context information (i.e., gray-building period) from rule use processing once contextual information was available (i.e., color-building period).

Behavioral Outcome Measures

Outcome measures were identical to those reported in Schwarb et al. (2015). All responses were categorized as context-correct (CC) if a placement was to the rule-correct side of the building or context-incorrect (CI) if a placement was to the rule-incorrect side. Studied face placements were further subcategorized as having been placed in the studied room or not resulting in four types of responses: CC-studied room (i.e., a room-correct/side-correct placement), CC-unstudied room (i.e., a room-incorrect/side-correct placement), CI-studied room (i.e., a room-correct/side-incorrect placement), and CI-unstudied room (i.e., a room-incorrect/side-incorrect placement).

Because this task was designed to dissociate the relational memory system and the memory-guided rule use system and because some types of responses were likely influenced by a single source of memory information (i.e., relational associations) whereas other types of responses were likely influenced by multiple sources of memory information (i.e., relational associations and contextual rule information), data were analyzed using three separate outcome metrics: (1) We assessed memory-guided rule use by evaluating the ability to use the extracted gender-by-side rule structure. For this analysis, only novel faces were considered. CC response provided a measure of memory-guided rule use independent of relational memory and is referred to as “novel accuracy.” (2) We assessed the shared contribution of relational memory and memory-guided rule use by evaluating CC-studied room responses (termed “target accuracy”). CC-studied room responses likely benefit both from relational memory success as well as rule knowledge, so disentangling these contributions is not possible using this measure. (3) We assessed relational memory by evaluating the preference for the CC-studied room over all CC responses (termed “target ratio”). This metric considers all responses for which the rule was applied and highlights those responses that were also specifically to the studied room, providing a measure of relational memory accounting for rule learning.

Statistical Analyses

Task performance on each behavioral measure of interest was compared with chance performance using one-sample t tests. Significance was determined at $p < .05$, and Cohen’s d is reported. Relationships between integrity of each DTI tract and behavioral outcome measures were calculated through bivariate correlations. Relationships between integrity of each MRE ROI and behavioral outcome measures were calculated through partial correlations controlling for age. Age was included as a covariate because it is known that MRE-derived measures of tissue integrity decrease with age beginning at 18 years of age (Arani et al., 2015; Sack, Streitberger, Krefting, Paul, & Braun, 2011; Sack et al., 2009) and the decline is greatest in the frontal lobes (Sack et al., 2011). Also, the vmPFC/OFC ROI

significantly correlated with age in our sample, $r = -.43$, $p = .033$. Relationships between regional volume and behavioral outcome measures were also calculated using partial correlations controlling for age because age significantly correlated with both hippocampal volume, $r = -.52$, $p = .019$, and vmPFC/OFC volume, $r = -.57$, $p = .007$, in our sample. Significance was determined at $p < .05$ for all correlations. Correlation coefficients for each brain–behavior pair were then compared by converting coefficients to z scores, calculating the asymptotic covariance, and computing a z statistic (Steiger, 1980). Given the nature of our hypotheses, one-tailed tests were considered when interpreting these data. fMRI statistical analyses in Experiment 2 are discussed below.

MRI Apparatus

In both experiments, images were acquired using a Siemens 3T TIM Trio whole-body MRI scanner. A standard 32-channel radio-frequency head coil was used and foam padding was used to restrict head motion. In Experiment 1, data were collected at the Biomedical Imaging Center at the Beckman Institute for Advanced Science and Technology at the University of Illinois. In Experiment 2, data were collected at the Center for Translational Imaging supported by the Northwestern University Department of Radiology at Northwestern University.

DTI Acquisition and Processing

High-resolution DTI data were acquired using a 3-D multi-slab, multishot spiral sequence designed to achieve high spatial resolution through optimized signal-to-noise efficiency and reduced distortion artifacts (Holtrop & Sutton, 2016; Johnson et al., 2014). Imaging parameters included 30 encoding directions at b value = 1000 sec/mm^2, 2 encodings at b value = 0 sec/mm^2, repetition time/echo time = 1875/82 msec, field of view = 240 × 240 mm^2, matrix = 150 × 150, 2 in-plane spiral shots (parallel imaging $R = 2$); 15 slabs with 4 slices per slab. The final image resolution was 1.6 × 1.6 × 1.6 mm^3 acquired in 8 min. Voxel-wise diffusion tensors were fit from diffusion-weighted images using FMRIB Diffusion Toolbox (Behrens et al., 2003) in FSL (Jenkinson, Beckmann, Behrens, Woolrich, & Smith, 2012), and fractional anisotropy (FA) was calculated.

To generate ROIs localized to specific tracts, we used two white matter atlases available in FSL (Hua et al., 2008; Mori et al., 2008). We created tract ROIs for individual subject data sets by first coregistering all FA maps to the MNI standard space through the nonlinear registration operation included in the Tract-Based Spatial Statistics tool (Smith et al., 2006). Inverse warp fields were then calculated and used to transform tract ROIs into subject space using FNIRT (Andersson, Smith, & Jenkinson, 2008).

The tracts investigated included the fimbria (i.e., the temporal or ventral portion of the fornix, which abuts the hippocampus and connects through the hypothalamus) and the UF; both tracts have been defined (Wendelken et al., 2015) and implicated in mnemonic processing (e.g., Wendelken et al., 2015; Douet & Chang, 2014; Sasson et al., 2013; Von Der Heide et al., 2013; Sexton et al., 2010; Rudebeck et al., 2009). We created ROIs from the core of each registered tract by thresholding the probabilistic maps at 20%. We computed the average FA across each ROI.

MRE Acquisition and Processing

The hippocampal elastography procedure for Experiment 1 has been reported (Schwarb et al., 2016). A pneumatic actuator (Resoundant, Rochester, MN) vibrated the brain at 50 Hz through a soft pad placed below the head. The resulting tissue deformation was encoded using a 3-D multislab, multishot spiral MRE sequence for capturing high-resolution displacement data so as to reduce partial volume effects and improve quantitative mechanical property estimation (Johnson et al., 2014). Tissue deformation was encoded using motion-sensitive gradients embedded in the sequence, which was repeated to capture motion along three separate axes and with opposite gradient polarities. We sampled the displacement fields at four points across one period of vibration, and the total acquisition time was 12 min. Imaging parameters included 1800/75 msec repetition/echo times, 240 mm^2 field of view, 150 × 150 imaging matrix, and sixty 1.6-mm-thick slices acquired in 10 overlapping slabs. Sampling within a slab used a stack of spirals, with two in-plane constant-density spiral readouts (Glover, 1999) and $R = 2$ SENSE parallel imaging factor (Pruessmann, Weiger, Börnert, & Boesiger, 2001). The resulting image volume had a 1.6 × 1.6 × 1.6 mm^3 isotropic voxel size, with 96 mm of coverage in the slab direction, which was aligned approximately AC–PC and included the MTL.

Bilateral hippocampal masks and bilateral vmPFC/OFC masks were generated from the acquired T1-weighted images using an MPRAGE sequence (magnetization-prepared rapid gradient echo; 0.9 × 0.9 × 0.9 mm^3 voxel size, 1900/900/2.32 msec repetition/inversion/echo times) using FreeSurfer v. 5.3 (Fischl et al., 2002). The hippocampal mask was generated from the Desikan–Killiany Atlas hippocampal parcellation, and the vmPFC/OFC mask was generated from the combination of the medial and lateral orbitofrontal labels (Morey, Haswell, Hooper, & De Bellis, 2016; Nopoulos et al., 2010; Boes et al., 2009).

Nonlinear inversion was used to estimate tissue viscoelasticity from MRE displacement data (McGarry et al., 2012). To improve the property estimates in subcortical regions, soft prior regularization (McGarry et al., 2013) promoted homogeneity in properties within the volume masks of the hippocampus. The mask was applied in native space by registration of the T1-weighted images to the MRE magnitude using FLIRT in FSL v. 5.0.7 (Jenkinson et al., 2012; Jenkinson, Bannister, Brady, & Smith, 2002). Nonlinear inversion estimates the complex shear modulus, $G = G' + iG''$, from which we determined the shear damping ratio, ξ. Damping ratio is a dimensionless quantity describing the relative attenuation level in the material (McGarry & Van Houten, 2008), defined as $\xi = G''/2G'$, and is similar to the viscoelastic phase angle often calculated in brain MRE (Guo et al., 2013; Lipp et al., 2013). $\xi \geq 1$ is known as critical damped or overdamped, where transient displacements will decay without oscillation. As in our previous work (Johnson et al., 2018; Schwarb et al., 2016, 2017), we report adjusted damping ratio, $\xi' = 1 - \xi$ to describe the relative elastic and viscous contributions to material behavior. Higher ξ' values indicate a more elastic solid, whereas lower ξ' values indicate a more viscous solid. As such, higher ξ' measures are indicative of greater tissue integrity.

Volume Acquisition and Processing

In Experiment 1, T1-weighted images using an MPRAGE sequence ($0.9 \times 0.9 \times 0.9$ mm^3 voxel size, 1900/900/2.32 msec repetition/inversion/echo times) were acquired, and FreeSurfer v. 5.3 (Fischl et al., 2002) was used to extract bilateral hippocampal and bilateral vmPFC/OFC volumes. All volumes were generated from the Desikan–Killiany Atlas. The hippocampal volume was determined by the automated hippocampal parcellation, and the vmPFC/OFC volume was determined by the combined automated medial and lateral orbitofrontal parcellations (e.g., Morey et al., 2016; Nopoulos et al., 2010; Boes et al., 2009). Automated measures of intracranial volume were also calculated (Buckner, 2004), and intracranial volume was used to normalize each ROI for head size (Erickson et al., 2009; Head, Kennedy, Rodrigue, & Raz, 2009; Raz et al., 2005).

fMRI Acquisition and Processing

In Experiment 2, an EPI sequence (repetition time = 2000 msec, echo time = 20 msec, flip angle = 80°, field of view = 220 mm) was used to acquire data sensitive to the BOLD signal. Each functional volume included thirty-five 3.0-mm axial slices. Each block lasted 7 min 10 sec (212 volumes/block). A high-resolution 3-D MPRAGE (inversion time = 1000 msec, flip angle = 8°) structural scan (1 mm isotropic voxels) was acquired at the end of the fMRI session. Stimuli were projected onto a screen and viewed through a mirror that was mounted on the head coil. Stimuli were shown, and data were collected using Presentation on a Windows-based computer. Participants responded using an MR-compatible roller ball mouse positioned comfortably across their lap.

Data reconstruction, processing, and analysis for each participant were performed in SPM12 (https://www.fil.ion.ucl.ac.uk/spm/software/spm12/). Images were slice time-corrected using the middle slice of each volume as a reference. Images were then spatially realigned and resliced to the first volume of the first block, and head motion artifacts were corrected to the first functional scan with a least squares approach using a six-parameter, rigid body transformation algorithm (Friston et al., 1995). Each MPRAGE was then coregistered to the mean EPI image for that participant. Data were normalized to MNI space with $3 \times 3 \times 3$ mm resolution and smoothed with a Gaussian filter (FWHM = 6 mm). Next, data were analyzed using a modified general linear model (Worsley & Friston, 1995). Only test phase data were analyzed. For each participant, a design matrix was created with the 18 covariates of interest (viz., studied faces: CC-studied room, CC-unstudied room, CI-studied room, CI-unstudied room trials; novel faces: CC and CI trials; in each of the face-only, gray-building, and color-building periods) convolved with an idealized hemodynamic response function. A high-pass filter removed frequencies below 0.0078 Hz. All analyses were performed during the retrieval period. For each participant, the following contrasts were performed. Face-only period: CC-studied room trials versus all novel face trials; activation from this contrast indicated regions that distinguished old from new faces (i.e., the standard old/new effect; for reviews, see Vilberg & Rugg, 2008; Wagner, Shannon, Kahn, & Buckner, 2005; Dobbins, Foley, Schacter, & Wagner, 2002). Gray-building period: CC-studied room trials versus all other studied face trials; during this period, participants are able to retrieve information about both rooms in which the given face had been studied (Schwarb et al., 2015) and activation from this contrast identified regions that support relational memory processing in

the absence of rule-relevant context information. Color-building period: rule-correct (CC novel and CC-unstudied room faces) trials versus CC-studied room trials; during this period, contextual information was revealed, and activation from this contrast identified regions that support the use of learned contextual rule information to guide the response.

Whole-brain statistical analyses were performed, and regional activation associated specifically with relational memory performance and memory-guided rule use were identified. So as to ensure that activity was specific to the contrast of interest in the period of interest (i.e., face-only, gray-building, or color-building), for each contrast of interest (e.g., CC-studied room trials vs. all novel face trials during the face-only period), exclusion masking was performed using the same contrast in the other two periods (e.g., CC-studied room trials vs. all novel face trials during both the gray-building and color-building periods) and a liberal uncorrected mask threshold of $p < .05$. This was done to exclude any voxels shared by any two periods and to ensure that activation clusters were unique to the period of interest. To correct for multiple comparisons at the whole-brain level, results were thresholded at $p < .001$, with a spatial extent of 26 continuous voxels, which is equivalent to a threshold of $p < .05$, corrected for multiple comparisons (Slotnick, Moo, Krauss, & Hart, 2003). This threshold was derived via Monte Carlo simulations, which included the following parameters: acquisition matrix = 128 × 128, 35 slices, original *xy* dimension voxel size = 1.7, original *z* dimension voxel size = 3, resampled voxel size = 3 mm, FWHM = 10.5, no mask, *p*-corrected, *p* voxel, iterations = 1000 (Slotnick, 2017). An anatomical hippocampus-specific ROI analysis was also performed. Parameter estimates from contrasts of interest were extracted and submitted to a one-sample *t* test.

RESULTS

Behavioral Outcomes

In Experiment 1, for studied faces, participants placed the face in the CC-studied room (i.e., target accuracy) on 58.3% (*SD* = 19.4%) of trials, a CC-unstudied room on 26.1% (*SD* = 14.2%) of trials, the CI-studied room on 5.0% (*SD* = 7.2%) of trials, and a CI-unstudied room on10.6% (*SD* = 11.1%) of trials. For novel faces, participants made a CC response on 81.4% (*SD* = 20.2%) of trials. In Experiment 2, for studied faces, participants placed the face in the CC-studied room on 47.0% (*SD* = 22.4%) of trials, a CC-unstudied room on 34.6% (*SD* = 11.7%) of trials, the CI-studied room on 5.8% (*SD* = 6.8%) of trials, and a CI-unstudied room on 12.6 (*SD* = 15.0%) of trials. For novel faces, participants made a CC response on 80.9% (*SD* = 15.5%) of trials.

Novel accuracy, target ratio, and target accuracy were the behavioral dependent measures of interest in both experiments. In Experiment 1, participants were very accurate, and the target ratio (i.e., measure of relational memory accounting for rule use) was 68.4% (*SD* =17.4%); this was significantly greater than chance given correct rule performance (11.1%), $t(19) = 14.68$, $p < .001$, $d = 3.29$. Target accuracy was on 58.3% (*SD* = 19.4%) and also significantly greater than chance (5.6%), $t(19) = 12.28$, $p < .001$, $d = 2.72$. Novel accuracy (i.e., measure or rule learning independent of relational memory) was 81.4% (*SD* = 20.2%) and significantly different from chance (50%), $t(19) = 6.94$, $p < .001$, $d = 1.55$. Target ratio and novel accuracy were not significantly correlated with each other, $r = .074$, $p = .757$; both

target ratio and target accuracy, $r = .823$, $p < .001$, and novel accuracy and target accuracy, $r = .454$, $p = .044$, were significantly correlated.

In Experiment 2, participants were again very accurate, and the target ratio was 54.5% and significantly greater than chance (11.1%), $t(19) = 9.55$, $p < .001$, $d = 2.14$. Target accuracy was 47.0% ($SD = 22.4\%$) and also significantly greater than chance (5.6%), $t(19) = 8.32$, $p < .001$, $d = 1.85$. Novel face accuracy was 81.1% and significantly different from chance (50%), $t(19) = 8.88$, $p < .001$, $d = 1.99$.

Structural Imaging Outcomes

In Experiment 1, the relationship between behavioral outcomes and the structural integrity of target ROIs were evaluated using both DTI and MRE.

DTI—First we consider the relationship between behavior and DTI-derived FA measures. We hypothesized that our relational memory measure (i.e., target ratio) would be related to fimbria, but not UF integrity. Indeed, fimbria FA (Figure 2) significantly correlated with target ratio ($r = .547$, $p = .007$), suggesting that fimbria integrity was sensitive to the correct studied location even among other rule-correct placements. The target ratio did not significantly correlate with UF integrity ($r = .054$, $p = .441$). Furthermore, these two correlations significantly differed from each other ($z = 1.81$, $p = .035$). We also hypothesized that our memory-guided rule use measure (i.e., novel accuracy) would be related to UF, but not fimbria tract integrity. Indeed, UF FA significantly correlated with novel accuracy ($r = .804$, $p < .001$). These data suggest that UF integrity is related to a participant's ability to successfully apply the learned rule information to novel, but related, situations. Conversely, fimbria FA did not significantly correlate with this measure of memory-guided rule use ($r = .369$, $p = .055$). These correlations were also significantly different from each other ($z = 2.17$, $p = .015$). Target accuracy significantly correlated with fimbria integrity ($r = .509$, $p = .011$), and the correlation with UF integrity approached significance ($r = .360$, $p = .060$). These two correlations were not significantly different from each other ($z = 0.57$, $p = .284$).

MRE—Next, we consider the relationship between behavior and MRE-derived viscoelasticity measures. We hypothesized that our relational memory measure (i.e., target accuracy) would be related to hippocampal viscoelasticity, but not vmPFC/OFC viscoelasticity. One participant was excluded from the analysis because their vmPFC/OFC viscoelasticity measure was a statistical outlier based on the conservative criterion of three times the median absolute deviation (Leys, Ley, Klein, Bernard, & Licata, 2013; Miller, 1991; Hampel, 1974). Data revealed a significant correlation between target ratio and hippocampal ξ' ($r = .401$, $p = .050$), but not vmPFC/OFC ξ' ($r = .062$, $p = .807$; Figure 3). The difference between these correlations approached significance ($z = 1.33$, $p = .091$). Next, we hypothesized that our memory-guided rule use measure (i.e., novel accuracy) would be related to vmPFC/OFC viscoelasticity, but not hippocampal viscoelasticity. Indeed vmPFC/OFC ξ' was significantly correlated with novel accuracy ($r = .511$, $p = .015$), but hippocampal ξ' was not ($r = .056$, $p = .412$). These correlations were significantly different from each other ($z = 1.87$, $p = .031$). Target accuracy significantly correlated with

hippocampal ξ′ (r = .414, p = .044), but not vmPFC/OFC ξ′ (r = .232, p = .175). These correlations did not significantly differ from each other (z = 0.73, p = .232).

Volume—The relationship between behavior and volume was also considered. One participant was excluded from the analysis because their hippocampal volume was a statistical outlier based on the conservative criterion of three times the median absolute deviation (Leys et al., 2013; Miller, 1991; Hampel, 1974). Target ratio was significantly correlated with hippocampal volume (r = .494, p = .019), but not vmPFC/OFC volume (r = −.087, p = .366). The difference between these correlations was significant (z = 2.16, p = .015). Target accuracy was not significantly correlated with either hippocampal volume (r = .159, p = .264) or vmPFC/OFC volume (r = −.028, p = .456). Finally, novel accuracy was not significantly correlated with either vmPFC/OFC volume accuracy (r = −.009, p = .486) or hippocampal volume (r = −.219, p = .192).

fMRI Outcomes

In Experiment 2, functional activation related to both relational memory processes and memory-guided rule use processes was investigated. Each test trial was divided into three different test periods (i.e., face-only, gray-building, and color-building), and each period allowed for a different hypothesis to be tested.

Face-only Period—During the face-only period of each test trial, no context (i.e., colored building) information was available so neither relational memory nor memory-guided rule use could be assessed. Participants could, however, determine whether or not the presented face had been studied or if it was novel (i.e., the standard old/new effect; for reviews, see Vilberg & Rugg, 2008; Wagner et al., 2005; Dobbins et al., 2002). The old/new effect was assessed by comparing CC-studied room trials (when the participant selected the correct room ensuring that they remembered seeing that face previously) to all novel faces (all trials with a nonstudied face). This contrast was then masked with the same contrast from the gray-building and color-building periods so that only those activation clusters unique to the face-only period were identified. Whole-brain analysis revealed activation in bilateral inferior parietal cortex and left ventrolateral pFC (Figure 4A; Table 1). These data replicate the standard old/new effect typical in the parietal (Vilberg & Rugg, 2008; Wagner et al., 2005) and prefrontal (Dulas & Duarte, 2012; Dobbins et al., 2002; Nolde, Johnson, & Raye, 1998) cortices. Distinguishing novel from studied faces is important when choosing where to place a novel face; if novel faces are not processed as new, a novel face might simply be mistaken for a studied face and placed in that studied face's location which would not require rule use.

Gray-building Period—Previous eye-tracking work using this task has shown that, during the gray-building period, participants recall the two possible locations in which the given face was studied, suggesting relational memory processing and hippocampal involvement (Schwarb et al., 2015). Additionally, Experiment 1 data suggest that hippocampal integrity is related to successful face placement in the correct room. As such, we predicted that the hippocampus would be active during the gray-building period for trials where participants would go on to correctly place a studied face in the correct room. To test this hypothesis,

activation from CC-studied room trials was compared with activation from all other studied face trials. There were no surviving voxels from the whole-brain analysis, and an anatomical hippocampal ROI analysis was performed. Parameter estimates for CC-studied room versus all other studied face trials contrast were extracted from the left and right hippocampus separately. Activation was significantly different from zero on the right, $t(19) = 2.25$, $p = .018$, but not the left, $t(19) = 1.08$, $p = .147$ (Figure 4B). Activation in left and right hippocampal ROIs in the face-only and color-building periods were not significantly different from zero ($p > .06$ in all cases).

Color-building Period—When context information was revealed, participants who had learned the underlying rule structure were able to use that information to correctly place faces on the CC side of the building. Data from Experiment 1 indicate that successful memory-guided rule use is related to UF/vmPFC/OFC integrity. To investigate the associated functional correlates, activity on trials where participants were likely to rely on their knowledge of the rule structure was contrasted with activity from trials where participants were likely to use relational memory processes. As such, rule-correct trials (i.e., both novel face trials in which there was no relational memory information to guide performance and studied face trials in which the correct room was not selected indicating a failure in relational memory, but accurate rule use) were contrasted with CC-studied room trials (where participants were most likely to rely on remembered relational information). This contrast was then exclusively masked with the same contrast from the face-only and gray-building periods. As predicted, activation was evident in the vmPFC/OFC (Figure 4C; Table 2).

DISCUSSION

The goal of this study was to investigate the shared and separable contributions of the MTL and pFC to memory performance. A context-dependent relational memory task designed to assess both relational memory as well as memory-guided rule use processes was implemented. A multimodality neuroimaging approach was applied, allowing us to explore these issues at multiple levels. DTI provided measures of white matter tract structural integrity, MRE provided measures of gray/white matter microstructural integrity, and fMRI provided measures of functional activation. Importantly, data from all three modalities converged into a coherent picture of MTL and pFC contributions to relational memory and memory-guided rule use. DTI, MRE, and fMRI each identified the hippocampus or hippocampal-adjacent fornix as essential for relational memory processing (i.e., selecting a correctly learned face–room association); similarly, each methodology also highlighted the importance of the vmPFC/OFC or UF (connecting vmPFC/OFC with MTL) as essential for memory-guided rule use processing (i.e., using a learned rule to guide performance with novel stimuli). These data add to the growing literature highlighting the importance of MTL–pFC interactions in support of mnemonic processing. They extend the previous work, however, by identifying dissociations among the contributions of MTL and pFC to successful performance on a single relational memory task. Furthermore, this structural dissociation emerged even among healthy young adults, emphasizing the power of sensitive behavioral tasks paired with sensitive neuroimaging measures. The data reported here cut

across previously independent literatures organized around individual imaging modalities to provide a more holistic account of the structure–function relationships contributing to context-dependent relational memory success, while also making specific contributions to each of these literatures.

There is a robust literature identifying a role for the fornix in support of mnemonic processing. In fact, the relationship between memory performance and fornix integrity has been established in patients with fornix re-section (e.g., Tsivilis et al., 2008), traumatic brain injury (e.g., Chang, Kim, Kim, Bai, & Jang, 2010), schizophrenia (e.g., Kuroki et al., 2006), and stroke (e.g., Hattingen et al., 2007) and among healthy older adults (e.g., Sasson et al., 2013). Specifically, the fornix seems critically involved in the formation of new memories (Sasson et al., 2013), such that damage to the fornix can result in profound antero-grade amnesia (Hattingen et al., 2007; Spiers, Maguire, & Burgess, 2001). Indeed, among healthy adults, DTI measures of fornix integrity show a significant relationship with episodic memory (for a review, see Douet & Chang, 2014), including successful recollection of spatial information (Rudebeck et al., 2009), behavioral pattern separation (Bennett & Stark, 2016; Bennett, Huffman, & Stark, 2015), and mnemonic control (i.e., controlled memory retrieval processes; Wendelken et al., 2015). Several studies have also specifically identified the fimbria portion of the fornix to be critical to mnemonic processing in healthy adults (Wendelken et al., 2015; Sexton et al., 2010; Rudebeck et al., 2009). Furthermore, fornix integrity has been tied to relational memory theory in that damage to the fornix in rats seems to impair memory formation only when flexible comparisons among multiple representations are required (e.g., Hudon, Dore, & Goulet, 2003; Eichenbaum, 1999; Eichenbaum, Fagan, Mathews, & Cohen, 1988; Dusek & Eichenbaum, 1997; Eichenbaum, Otto, & Cohen, 1994; Cohen & Eichenbaum, 1991); similar results have also been reported in nonhuman primates with fornix damage (Buckmaster, Eichenbaum, Amaral, Suzuki, & Rapp, 2004). The current work supports and extends previous work highlighting the role of the fornix in successful relational memory processing in healthy young adults.

The contribution of the UF to mnemonic processing is less consistently reported. The UF is thought to be important in the formation and retrieval of memories (Sasson et al., 2013); however, data suggest UF integrity does not influence all aspects of memory, but rather its role is highly specific (Von Der Heide et al., 2013). For example, nonhuman primates with damaged UF show normal delayed match to sample performance and normal stimulus–reward associations across a delay (Gaffan, Easton, & Parker, 2002; Parker & Gaffan, 1998; Gutnikov, Ma, Buckley, & Gaffan, 1997). However, in humans, UF integrity is associated with performance on delayed story recall among patients with mild cognitive impairment (Fujie et al., 2008), source memory performance in a group of older adults (Lockhart et al., 2012), and delayed word recall in a group of traumatic brain injury patients (Niogi et al., 2008). UF integrity has also been shown to be essential for mnemonic control among older adults and children (Wendelken et al., 2015). Recently, in an effort to review and organize the literature concerning mnemonic processing and UF integrity, Von Der Heide et al. (2013) noted that conditional rule learning is the only type of mnemonic processing consistently impaired following UF damage, and they proposed a unifying theory of UF function in memory. They suggest that the role of the UF is to allow memory representations (viz. temporal lobe mnemonic associations) to modify behavior via valence-based biasing of

decisions (viz. orbital frontal stimulus–reward associations). The current data are also consistent with this framework. In the context-dependent relational memory task, participants can use consistencies in information from individual face–room pairs to extract the underlying gender-by-side rule structure. Although explicit valence-laden feedback is not provided in this task, consistent repetitions during study allow for participants to self-test their memory for individual pairs, and participants are also provided with the correct pairing with each repetition (Schwarb et al., 2015). These data suggest that the UF, which supports bidirectional communication between MTL and pFC, contributes to this sort of iterative mnemonic processing.

Exploring structure–function relationships using MRE is an emerging research area. The underlying cytoarchitectural characteristics that contribute to viscoelasticity measures are not well defined; however, it is generally believed that the damping ratio measure (ξ) reflects the organization and complexity of the underlying brain tissue components (Johnson et al., 2013; Sack, Johrens, Wurfel, & Braun, 2013; Schregel et al., 2012) and is likely related to the integrity of the extracellular matrix (Schregel et al., 2012), although there are likely other contributing factors as well. Considerably more work combining both in vivo MRE and ex vivo histology is essential to bridge this gap. Still, it is understood that MRE measures reflect some aspects of microstructural tissue integrity and work with healthy young adults suggests that there are microstructural differences, even in this population, that are meaningful for cognitive outcomes (Johnson et al., 2018; Schwarb et al., 2016, 2017). For this reason, MRE appears to be a useful tool for investigating regional integrity across the lifespan and may be particularly useful for healthy young adults for whom other structural measures, like volume, have so far been less informative. Decline in brain viscoelasticity with typical aging (Hiscox, Johnson, McGarry, Perrins, et al., 2018; Arani et al., 2015; Sack et al., 2011) as well as differences in viscoelasticity among healthy individuals and patients with neurodegenerative disorders such as multiple sclerosis (Sandroff, Johnson, & Motl, 2017; Streitberger et al., 2012), Alzheimer's disease (Munder et al., 2018; Murphy et al., 2011, 2016), and amyotrophic lateral sclerosis (Romano et al., 2014) are frequently reported. Although all of these populations typically show cognitive deficits as well, there have been few studies directly evaluating the relationship between MRE-derived microstructural integrity and cognition (for a review, see Murphy, Huston, & Ehman, 2017). That said, there is a growing body of literature investigating the specific relationship between hippocampal viscoelasticity and episodic memory. Indeed MRE-derived measures of hippocampal integrity show a positive relationship with word recall performance in multiple sclerosis patients (i.e., episodic memory; Sandroff et al., 2017), paired associate memory among healthy older adults (Hiscox, Johnson, McGarry, Schwarb, et al., 2018), as well spatial reconstruction performance among healthy young adults (i.e., relational memory; Johnson et al., 2018; Schwarb et al., 2016, 2017), such that individuals with a more elastic hippocampus perform better on memory tasks. The current data are consistent with these findings but also extend this relationship to a new measure of relational memory among healthy young adults (previous investigations have all used the spatial reconstruction task); a significant contribution to the understanding of relational memory processes, rather than specific task performance, and hippocampal viscoelasticity. To date, investigations of viscoelastic

contributions to memory performance have been restricted to the hippocampus, and these data provide the first extension to other structures, namely, vmPFC/OFC.

In these two experiments, we consistently report a dissociation between the hippocampus and vmPFC/OFC in supporting relational memory retrieval and memory-guided rule use. Previous studies have identified a role for the MTL in rule/pattern learning similar to that of the pFC (e.g., Seger & Cincotta, 2006; Schendan, Searl, Melrose, & Stern, 2003; Rose, Haider, Weiller, & Buchel, 2002; Grafton, Hazeltine, & Ivry, 1995). Those studies, however, have focused specifically on the encoding period and have noted that hippocampal involvement in rule learning only occurs early in the learning episode (Seger & Cincotta, 2006). Related recent work has demonstrated that posterior hippocampus is important for keeping distinct representations separate in memory whereas the anterior hippocampus is important for integrating information across memories (Schlichting, Mumford, & Preston, 2015). It is entirely possible that the hippocampus, specifically anterior hippocampus, participates in rule learning in the current task as well; however, the task was not designed to assess the learning/encoding phase, and therefore, this possibility cannot be investigated with the existing data.

Volume is often too coarse a metric to identify meaningful relationships with cognition in a sample of healthy young adults for whom atrophy is not yet evident and, in fact, significant relationships between volume and cognitive performance are not typically reported in such samples (e.g., Schwarb et al., 2016, 2017). For this reason, it is unsurprising that the relationships investigated here, with one exception, were not significant. We have previously reported a significant positive relationship between target ratio and hippocampal volume in a sample of healthy older adults (Schwarb et al., 2015) and that relationship was replicated here. That previous report also identified a negative correlation with vmPFC volume and novel accuracy; however, that relationship was not replicated in this sample. The directionality of that finding, individuals with smaller vmPFC volumes made more rule-consistent responses with novel faces, was interpreted as the consequence of a tradeoff particular to older adults. In that sample, individuals with the lowest novel accuracy made more CI-studied room responses (note that CI-studied room responses were quite rare [5%] in the current investigation), suggesting that they ignored the contextual rule in favor of learning the contextually inaccurate face–room association.

Functional neuroimaging studies also provide evidence for the role of both vmPFC and MTL in memory processing (e.g., Zeithamova, Dominick, et al., 2012; Bunge et al., 2004); however, researchers are still seeking to understand the interdependencies between and the mechanisms governing their interactions. fMRI investigations of relational memory processing complement decades of patient research, indicating that the hippocampus is active when relational memory processes are engaged (e.g., Hannula, Libby, Yonelinas, & Ranganath, 2013; Voss et al., 2011; Zalesak & Heckers, 2009; Hannula & Ranganath, 2008; Heckers, Zalesak, Weiss, Ditman, & Titone, 2004). For example, Hannula and Ranganath (2008) asked participants to study different arrangements of objects on a computer screen; after a short delay, the objects reappeared either in a matching or mismatching configuration. The hippocampus was more active for match trials where the relational information was intact compared with mismatch trials. Although the hippocampus is essential for relational

memory processing, the vmPFC is involved in guiding memory retrieval of hippocampal-generated representations to select the appropriate representation in a given context (Rubin et al., 2017; Gershman et al., 2015; Wang et al., 2015; Preston & Eichenbaum, 2013; Kroes & Fernandez, 2012). For example, Kalisch et al. (2006) conducted an experiment in which extinction of a fear-conditioned stimulus was tied to a particular experimental context. Context-dependent recall of the extinction memory activated the left vmPFC and also the left anterior hippocampus. Current theories posit that both the MTL and pFC, as well as their interaction, are essential for memory integration and the formation of context-dependent representations, which then allows for flexible inference to novel situations (Schlichting & Preston, 2015; Wang et al., 2015; Preston & Eichenbaum, 2013; Miller & Cohen, 2001). Indeed, in a transitive inference test, successful inference performance correlates with both hippocampus and vmPFC fMRI activation, and hippocampus–vmPFC connectivity increases with multiple repetitions of overlapping episodes (Zeithamova, Dominick, et al., 2012). Interestingly, hippocampal lesion patients are impaired on learning both the premise and inference pairs in this task (Smith & Squire, 2005), whreas vmPFC/OFC lesion patients are impaired only on the inference pairs (Spalding et al., 2018). The current data complement these earlier findings, highlighting related but not identical roles for vmPFC/OFC and hippocampus in supporting mnemonic behavior. Given the current data and the existing literature, we propose an interactive view of hippocampal and vmPFC/OFC contributions to context-dependent memory. In this view, the hippocampus is necessary to bind arbitrary pieces of information into a coherent relational memory representation and also necessary when those learned representations are later retrieved. The vmPFC/OFC is able to extract regularities/rules from the hippocampally generated relational memory representations and is engaged when learned rule information is applied to shape future behavior. Memory-guided rule use emerges as an output from accruing remembered information.

Small sample sizes in neuroscience raise important concerns regarding statistical power and the overestimates of real effects (for a review, see Button et al., 2013). Data from 20 participants are reported in Experiment 1, and the observed effect sizes were consistent with all other reported effect sizes comparing hippocampal ξ' to memory processes (Hiscox, Johnson, McGarry, Schwarb, et al., 2018; Johnson et al., 2018; Schwarb et al., 2016, 2017). To date, sample sizes in the emerging MRE literature have been small, so it is possible that these large effect sizes are an overestimate of the true effect size in the population and future work with larger samples will be essential for determining the true effect size of these relationships. Importantly for the current study, in addition to correlations, significant region by task interactions of correlations are also reported, which are less likely to result in a spurious finding than a single correlation (Nieuwenhuis, Forstmann, & Wagenmakers, 2011). As we have noted previously (Johnson et al., 2018; Schwarb et al., 2016, 2017), MRE appears to provide sensitive measures of structural integrity that are related to cognitive processes and that consistently outperform volumetric measures among healthy young adults. Small sample fMRI investigations have also recently been challenged, and valid and important points have been made on this topic (Turner, Paul, Miller, & Barbey, 2018; Poldrack et al., 2017). Although the sample size in the current fMRI experiment is indeed small ($N = 20$), the data complement and mirror the findings from Experiment 1. We propose that there is considerable strength in using multiple and converging methods to

address the same hypotheses, particularly across different samples. In this investigation, data from DTI, MRE, and fMRI in two naïve groups of participants all support the conclusion that the hippocampus contributes to relational memory processing whereas the vmPFC/OFC contributes to memory-guided rule use. Therefore, although it is possible that any one modality produced a false positive result, the fact that all three methods support the same findings, we believe, is compelling and lends credence to the veracity of the findings despite the small sample size.

A limitation of Experiment 1 is that only male participants were included, and as such, data should be interpreted accordingly and not generalized to the greater population. The presented data set was the first ever collected to include both MRE and cognitive measures and because of known sex differences in MRE measures of the brain (Sack et al., 2009), particularly in the temporal lobes (Arani et al., 2015), a cautious approach was adopted and only men were included. Future studies must, of course, include both men and women, as the current data only speak to the relationship between microstructural integrity and cognitive outcomes in half of the population. This next step is essential in establishing MRE as a tool to probe cognition. To this end, since the acquisition of these data, all subsequent studies have included both men and women (Johnson et al., 2018; Schwarb et al., 2017), and furthermore, we are currently running a new large-scale study to specifically investigate sex effects on MRE, cognitive outcomes, and their interactions.

Conclusions

Current memory theories posit that mnemonic processing is supported not by a single structure but by a dynamic memory system composed of multiple regions throughout the brain. This investigation focused on two important hubs in this network, MTL and pFC, known to support relational memory processes (Wang et al., 2015; Preston & Eichenbaum, 2013; Eichenbaum & Cohen, 2001; Cohen & Eichenbaum, 1993). The data reported here suggest that, although both MTL and pFC structures contribute to successful relational memory task performance, they each uniquely contribute to successful behavioral outcomes. MTL structures are essential for forming relational memory representations, whereas vmPFC/OFC structures, and their connections with the MTL, are essential for abstracting regularities from learned associations to support flexible and conditional behavior when presented with new information. Importantly, these structure–function relationships were consistent across three separate neuroimaging methods highlighting the stability of the relationships regardless of the imaging modality applied.

Acknowledgments

NIH/NIMH grant R01-MH062500 and the Biomedical Imaging Center of the Beckman Institute at the University of Illinois provided partial support for the work presented in Experiment 1. Experiment 1 was carried out in part at the Biomedical Imaging Center of the Beckman Institute for Advanced Science and Technology at the University of Illinois. NIH/NIMH grant R01-MH062500 and Silvio O. Conte Center Award MH094263 provided partial support for the work presented in Experiment 2. Experiment 2 was carried out in part at the Center for Translational Imaging, supported by the Northwestern University Department of Radiology. We would also like to thank Elise Gagnon for her assistance in recruiting participants for the fMRI study and Rebecca Golden for her assistance in creating hippocampal masks for the MRE study.

REFERENCES

Althoff RR, & Cohen NJ (1999). Eye-movement-based memory effect: A reprocessing effect in face perception. Journal of Experimental Psychology: Learning, Memory, and Cognition, 25, 997–1010.

American Psychological Association. (1992). Ethical principles of psychologists and code of conduct. American Psychologist, 47, 1597–1611.

Andersson J, Smith SM, & Jenkinson M (2008). FNIRT – FMRIB's non-linear image registration tool. Paper presented at the Fourteenth Annual Meeting of the Organization for Human Brain Mapping, Melbourne, Australia.

Arani A, Murphy MC, Glaser KJ, Manduca A, Lake DS, Kruse SA, et al. (2015). Measuring the effects of aging and sex on regional brain stiffness with MR elastography in healthy older adults. Neuroimage, 111, 59–64. [PubMed: 25698157]

Badre D, & Nee DE (2018). Frontal Cortex and the Hierarchical Control of Behavior. Trends in Cognitive Sciences, 22, 170–188. [PubMed: 29229206]

Battaglia FP, Benchenane K, Sirota A, Pennartz CM, & Wiener SI (2011). The hippocampus: Hub of brain network communication for memory. Trends in Cognitive Sciences, 15, 310–318. [PubMed: 21696996]

Behrens TE, Woolrich MW, Jenkinson M, Johansen-Berg H, Nunes RG, Clare S, et al. (2003). Characterization and propagation of uncertainty in diffusion-weighted MR imaging. Magnetic Resonance in Medicine, 50, 1077–1088. [PubMed: 14587019]

Bennett IJ, Huffman DJ, & Stark CE (2015). Limbic tract integrity contributes to pattern separation performance across the lifespan. Cerebral Cortex, 25, 2988–2999. [PubMed: 24825784]

Bennett IJ, & Stark CE (2016). Mnemonic discrimination relates to perforant path integrity: An ultra-high resolution diffusion tensor imaging study. Neurobiology of Learning and Memory, 129, 107–112. [PubMed: 26149893]

Boes AD, Bechara A, Tranel D, Anderson SW,Richman L, & Nopoulos P (2009). Right ventromedial prefrontal cortex: A neuroanatomical correlate of impulse control in boys. Social Cognitive and Affective Neuroscience, 4, 1–9. [PubMed: 19015086]

Buckmaster CA, Eichenbaum H, Amaral DG, Suzuki WA, & Rapp PR (2004). Entorhinal cortex lesions disrupt the relational organization of memory in monkeys. Journal of Neuroscience, 24, 9811–9825. [PubMed: 15525766]

Buckner RL (2003). Functional-anatomic correlates of control processes in memory. Journal of Neuroscience, 23, 3999–4004. [PubMed: 12764084]

Buckner RL (2004). Memory and executive function in aging and AD: Multiple factors that cause decline and reserve factors that compensate. Neuron, 44, 195–208. [PubMed: 15450170]

Bunge SA, Burrows B, & Wagner AD (2004). Prefrontal and hippocampal contributions to visual associative recognition: Interactions between cognitive control and episodic retrieval. Brain and Cognition, 56, 141–152. [PubMed: 15518931]

Button KS, Ioannidis JP, Mokrysz C, Nosek BA, Flint J, Robinson ES, et al. (2013). Power failure: Why small sample size undermines the reliability of neuroscience. Nature Reviews Neuroscience, 14, 365–376. [PubMed: 23571845]

Chang MC, Kim SH, Kim OL, Bai DS, & Jang SH (2010). The relation between fornix injury and memory impairment in patients with diffuse axonal injury: A diffusion tensor imaging study. Neurorehabilitation, 26, 347–353. [PubMed: 20555158]

Cohen NJ (2015). Navigating life. Hippocampus, 25, 704–708. [PubMed: 25787273]

Cohen NJ, & Eichenbaum H (1991). The theory that wouldn't die: A critical look at the spatial mapping theory of hippocampal function. Hippocampus, 1, 265–268. [PubMed: 1669304]

Cohen NJ, & Eichenbaum H (1993). Memory, amnesia and the hippocampal system. Cambridge, MA: MIT Press.

Dobbins IG, Foley H, Schacter DL, & Wagner AD (2002). Executive control during episodic retrieval: Multiple prefrontal processes subserve source memory. Neuron, 35, 989–996. [PubMed: 12372291]

Douet V, & Chang L (2014). Fornix as an imaging marker for episodic memory deficits in healthy aging and in various neurological disorders. Frontiers in Aging Neuroscience, 6, 343. [PubMed: 25642186]

Dulas MR, & Duarte A (2012). The effects of aging on material-independent and material-dependent neural correlates of source memory retrieval. Cerebral Cortex, 22, 37–50. [PubMed: 21616984]

Dusek JA, & Eichenbaum H (1997). The hippocampus and memory for orderly stimulus relations. Proceedings of the National Academy of Sciences, U.S.A, 94, 7109–7114.

Eichenbaum H (1999). The hippocampus and mechanisms of declarative memory. Behavioural Brain Research, 103, 123–133. [PubMed: 10513581]

Eichenbaum H, & Cohen NJ (2001). From conditioning to conscious recollection: Multiple memory systems in the brain. New York, NY: Oxford University Press.

Eichenbaum H, & Cohen NJ (2014). Can we reconcile the declarative memory and spatial navigation views on hippocampal function? Neuron, 83, 764–770. [PubMed: 25144874]

Eichenbaum H, Fagan A, Mathews P, & Cohen NJ (1988). Hippocampal system dysfunction and odor discrimination learning in rats: Impairment or facilitation depending on representational demands. Behavioral Neuroscience, 102, 331–339. [PubMed: 3395444]

Eichenbaum H, Otto T, & Cohen NJ (1994). Two functional components of the hippocampal memory system. Behavioral and Brain Sciences, 17, 449–517.

Eichenbaum H, Yonelinas AP, & Ranganath C (2007). The medial temporal lobe and recognition memory. Annual Review of Neuroscience, 30, 123–152.

Erickson KI, Prakash RS, Voss MW, Chaddock L, Hu L, Morris KS, et al. (2009). Aerobic fitness is associated with hippocampal volume in elderly humans. Hippocampus, 19, 1030–1039. [PubMed: 19123237]

Fischl B, Salat DH, Busa E, Albert M, Dieterich M, Haselgrove C, et al. (2002). Whole brain segmentation: Automated labeling of neuroanatomical structures in the human brain. Neuron, 33, 341–355. [PubMed: 11832223]

Friston KJ, Ashburner J, Frith CD, Poline JB, Heather JD, & Frackowiak RSJ (1995). Spatial registration and normalization of images. Human Brain Mapping, 3, 165–189.

Fujie S, Namiki C, Nishi H, Yamada M, Miyata J, Sakata D, et al. (2008). The role of the uncinate fasciculus in memory and emotional recognition in amnestic mild cognitive impairment. Dementia and Geriatric Cognitive Disorders, 26, 432–439. [PubMed: 18957848]

Gaffan D, Easton A, & Parker A (2002). Interaction of inferior temporal cortex with frontal cortex and basal forebrain: Double dissociation in strategy implementation and associative learning. Journal of Neuroscience, 22, 7288–7296. [PubMed: 12177224]

Gershman SJ, Norman KA, & Niv Y (2015). Discovering latent causes in reinforcement learning. Current Opinion in Behavioral Sciences, 5, 43–50.

Glover GH (1999). Simple analytic spiral K-space algorithm.Magnetic Resonance in Medicine, 42, 412–415. [PubMed: 10440968]

Grafton ST, Hazeltine E, & Ivry R (1995). Functional mapping of sequence learning in normal humans. Journal of Cognitive Neuroscience, 7, 497–510. [PubMed: 23961907]

Guo J, Hirsch S, Fehlner A, Papazoglou S, Scheel M,Braun J, et al. (2013). Towards an elastographic atlas of brain anatomy. PLoS One, 8, e71807. [PubMed: 23977148]

Gutnikov SA, Ma YY, Buckley MJ, & Gaffan D (1997). Monkeys can associate visual stimuli with reward delayed by 1 s even after perirhinal cortex ablation, uncinate fascicle section or amygdalectomy. Behavioural Brain Research, 87, 85–96. [PubMed: 9331476]

Hampel FR (1974). The influence curve and its role in robust estimation. Journal of the American Statistical Association, 69, 383–393.

Hannula DE, Libby LA, Yonelinas AP, & Ranganath C (2013). Medial temporal lobe contributions to cued retrieval of items and contexts. Neuropsychologia, 51, 2322–2332. [PubMed: 23466350]

Hannula DE, & Ranganath C (2008). Medial temporal lobe activity predicts successful relational memory binding. Journal of Neuroscience, 28, 116–124. [PubMed: 18171929]

Hattingen E, Rathert J, Raabe A, Anjorin A, Lanfermann H,& Weidauer S (2007). Diffusion tensor tracking of fornix infarction. Journal of Neurology, Neurosurgery, and Psychiatry, 78, 655–656.

Head D, Kennedy KM, Rodrigue KM, & Raz N (2009). Age differences in perseveration: Cognitive and neuroanatomical mediators of performance on the Wisconsin card sorting test. Neuropsychologia, 47, 1200–1203. [PubMed: 19166863]

Heckers S, Zalesak M, Weiss AP, Ditman T, & Titone D (2004). Hippocampal activation during transitive inference in humans. Hippocampus, 14, 153–162. [PubMed: 15098721]

Hiscox LV, Johnson CL, McGarry MDJ, Perrins M, Littlejohn A, van Beek EJR, et al. (2018). High-resolution magnetic resonance elastography reveals differences in subcortical gray matter viscoelasticity between young and healthy older adults. Neurobiology of Aging, 65, 158–167. [PubMed: 29494862]

Hiscox LV, Johnson CL, McGarry MDJ, Schwarb H, van Beek EJR, Roberts N, et al. (2018). Hippocampal viscoelasticity and episodic memory performance in healthy older adults examined with magnetic resonance elastography. Brain Imaging and Behavior. 10.1007/s11682-018-9988-8.

Holtrop JL, & Sutton BP (2016). Pushing the bounds of high-resolution diffusion weighted imaging on clinical 3 T MRI scanners using multi-slab spiral acquisitions. Journal of Medical Imaging, 3, 023501. [PubMed: 27088107]

Hua K, Zhang J, Wakana S, Jiang H, Li X, Reich DS, .et al.(2008). Tract probability maps in stereotaxic spaces: Analyses of white matter anatomy and tract-specific quantification. Neuroimage, 39, 336–347. [PubMed: 17931890]

Hudon C, Dore FY, & Goulet S (2003). Selective impairment of fornix-transected rats on a new nonspatial, odor-guided task. Hippocampus, 13, 48–52. [PubMed: 12625456]

Jenkinson M, Bannister PR, Brady M, & Smith SM (2002).Improved optimization for the robust and accurate linear registration and motion correction of brain images. Neuroimage, 17, 825–841. [PubMed: 12377157]

Jenkinson M, Beckmann CF, Behrens TE, Woolrich MW, & Smith SM (2012). FSL. Neuroimage, 62, 782–790. [PubMed: 21979382]

Johnson CL, Holtrop JL, McGarry MD, Weaver JB, Paulsen KD, Georgiadis JG, et al. (2014). 3D multislab, multishot acquisition for fast, whole-brain MR elastography with high signal-to-noise efficiency. Magnetic Resonance in Medicine, 71, 477–485. [PubMed: 24347237]

Johnson CL, McGarry MD, Gharibans AA, Weaver JB, Paulsen KD, Wang H, et al. (2013). Local mechanical properties of white matter structures in the human brain. Neuroimage, 79, 145–152. [PubMed: 23644001]

Johnson CL, Schwarb H, Horecka KM, McGarry MDJ, Hillman CH, Kramer AF, et al. (2018). Double dissociation of structure-function relationships in memory and fluid intelligence observed with magnetic resonance elastography. Neuroimage, 171, 99–106. [PubMed: 29317306]

Johnson CL, Schwarb H, McGarry MDJ, Anderson AT, Huesmann GR, Sutton BP, et al. (2016). Viscoelasticity of subcortical gray matter structures. Human Brain Mapping, 37, 4221–4233. [PubMed: 27401228]

Kalisch R, Korenfeld E, Stephan KE, Weiskopf N,Seymour B, & Dolan RJ (2006). Context-dependent human extinction memory is mediated by a ventromedial prefrontal and hippocampal network. Journal of Neuroscience, 26, 9503–9511. [PubMed: 16971534]

Konkel A, & Cohen NJ (2009). Relational memory and the hippocampus: Representations and methods. Frontiers in Neuroscience, 3, 166–174. [PubMed: 20011138]

Kroes MC, & Fernandez G (2012). Dynamic neural systems enable adaptive, flexible memories. Neuroscience and Biobehavioral Reviews, 36, 1646–1666. [PubMed: 22874579]

Kuroki N, Kubicki M, Nestor PG, Salisbury DF, Park HJ, Levitt JJ, et al. (2006). Fornix integrity and hippocampal volume in male schizophrenic patients. Biological Psychiatry, 60, 22–31. [PubMed: 16406249]

Leys C, Ley C, Klein O, Bernard P, & Licata L (2013).Detecting outliers: Do not use standard deviation around the mean, use absolute deviation around the median. Journal of Experimental Social Psychology, 49, 764–766.

Lipp A, Trbojevic R, Paul F, Fehlner A, Hirsch S, Scheel M, et al. (2013). Cerebral magnetic resonance elastography in supranuclear palsy and idiopathic Parkinson's disease. Neuroimage: Clinical, 3, 381–387. [PubMed: 24273721]

Lockhart SN, Mayda AB, Roach AE, Fletcher E,Carmichael O, Maillard P, et al. (2012). Episodic memory function is associated with multiple measures of white matter integrity in cognitive aging. Frontiers in Human Neuroscience, 6, 56. [PubMed: 22438841]

Maguire EA, & Mullally SL (2013). The hippocampus: A manifesto for change. Journal of Experimental Psychology: General, 142, 1180–1189. [PubMed: 23855494]

McGarry MDJ, Johnson CL, Sutton BP, Van Houten EEW, Georgiadis JG, Weaver JB, et al. (2013). Including spatial information in nonlinear inversion MR elastography using soft prior regularization. IEEE Transactions on Medical Imaging, 32, 1901–1909. [PubMed: 23797239]

McGarry MDJ, & Van Houten EEW (2008). Use of a Rayleigh damping model in elastography. Medical & Biological Engineering & Computing, 46, 759–766. [PubMed: 18521645]

McGarry MDJ, Van Houten EEW, Johnson CL, Georgiadis JG, Sutton BP, Weaver JB, et al. (2012). Multiresolution MR elastography using nonlinear inversion. Medical Physics, 39, 6388–6396. [PubMed: 23039674]

Miller J (1991). Reaction time analysis with outlier exclusion:Bias varies with sample size. Quarterly Journal of Experimental Psychology, 43, 907–912. [PubMed: 1775668]

Miller EK (1999a). Straight from the top. Nature, 401,650–651. [PubMed: 10537100]

Miller EK (1999b). The prefrontal cortex: Complex neural properties for complex behavior. Neuron, 22, 15–17. [PubMed: 10027284]

Miller EK, & Cohen JD (2001). An integrative theory of prefrontal cortex function. Annual Review of Neuroscience, 24, 167–202.

Miller EK, Freedman DJ, & Wallis JD (2002). The prefrontal cortex: Categories, concepts and cognition. Philosophical Transactions of the Royal Society of London, Series B: Biological Sciences, 357, 1123–1136. [PubMed: 12217179]

Monti JM, Cooke GE, Watson PD, Voss MW, Kramer AF, & Cohen NJ (2015). Relating hippocampus to relational memory processing across domains and delays. Journal of Cognitive Neuroscience, 27, 234–245. [PubMed: 25203273]

Morey RA, Haswell CC, Hooper SR, & De Bellis MD (2016). Amygdala, hippocampus, and ventral medial prefrontal cortex volumes differ in maltreated youth with and without chronic posttraumatic stress disorder. Neuropsychopharmacology, 41, 791–801. [PubMed: 26171720]

Mori S, Oishi K, Jiang H, Jiang L, Li X, Akhter K, et al. (2008). Stereotaxic white matter atlas based on diffusion tensor imaging in an ICBM template. Neuroimage, 40, 570–582. [PubMed: 18255316]

Moscovitch M, Cabeza R, Winocur G, & Nadel L (2016). Episodic memory and beyond: The hippocampus and neocortex in transformation. Annual Review of Psychology, 67, 105–134.

Munder T, Pfeffer A, Schreyer S, Guo J, Braun J, Sack I, et al. (2018). MR elastography detection of early viscoelastic response of the murine hippocampus to amyloid beta accumulation and neuronal cell loss due to Alzheimer's disease. Journal of Magnetic Resonance Imaging, 47, 105–114. [PubMed: 28422391]

Murphy MC, Huston J III, & Ehman RL (2017). MR elastography of the brain and its application in neurological diseases. Neuroimage, 187, 176–183. [PubMed: 28993232]

Murphy MC, Huston J III, Jack CR Jr., Glaser KJ, Manduca A, Felmlee JP, et al. (2011). Decreased brain stiffness in Alzheimer's disease determined by magnetic resonance elastography. Journal of Magnetic Resonance Imaging, 34, 494–498. [PubMed: 21751286]

Murphy MC, Jones DT, Jack CR Jr., Glaser KJ, Senjem ML, Manduca A, et al. (2016). Regional brain stiffness changes across the Alzheimer's disease spectrum. Neuroimage: Clinical, 10, 283–290. [PubMed: 26900568]

Nieuwenhuis S, Forstmann BU, & Wagenmakers EJ (2011). Erroneous analyses of interactions in neuroscience: A problem of significance. Nature Neuroscience, 14, 1105–1107. [PubMed: 21878926]

Niogi SN, Mukherjee P, Ghajar J, Johnson CE, Kolster R, Lee H, et al. (2008). Structural dissociation of attentional control and memory in adults with and without mild traumatic brain injury. Brain, 131, 3209–3221. [PubMed: 18952679]

Nolde SF, Johnson MK, & Raye CL (1998). The role of prefrontal cortex during tests of episodic memory. Trends in Cognitive Sciences, 2, 399–406. [PubMed: 21227255]

Nopoulos P, Boes AD, Jabines A, Conrad AL, Canady J, Richman L, et al. (2010). Hyperactivity, impulsivity, and inattention in boys with cleft lip and palate: Relationship to ventromedial prefrontal cortex morphology. Journal of Neurodevelopmental Disorders, 2, 235–242. [PubMed: 22127933]

Parker A, & Gaffan D (1998). Memory after frontal/temporal disconnection in monkeys: Conditional and non-conditional tasks, unilateral and bilateral frontal lesions. Neuropsychologia, 36, 259–271. [PubMed: 9622191]

Poldrack RA, Baker CI, Durnez J, Gorgolewski KJ,Matthews PM, Munafo MR, et al. (2017). Scanning the horizon: Towards transparent and reproducible neuroimaging research. Nature Reviews Neuroscience, 18, 115–126. [PubMed: 28053326]

Preston AR, & Eichenbaum H (2013). Interplay of hippocampus and prefrontal cortex in memory. Current Biology, 23, R764–R773. [PubMed: 24028960]

Price G, Cercignani M, Parker GJ, Altmann DR, Barnes TR, Barker GJ, et al. (2008). White matter tracts in first-episode psychosis: A DTI tractography study of the uncinate fasciculus. Neuroimage, 39, 949–955. [PubMed: 17988894]

Pruessmann KP, Weiger M, Börnert P, & Boesiger P (2001). Advances in sensitivity encoding with arbitrary k-space trajectories. Magnetic Resonance in Medicine, 46, 638–651. [PubMed: 11590639]

Ranganath C (2010). A unified framework for the functional organization of the medial temporal lobes and the phenomenology of episodic memory. Hippocampus, 20, 1263–1290. [PubMed: 20928833]

Ranganath C, Heller A, Cohen MX, Brozinsky CJ, & Rissman J (2005). Functional connectivity with the hippocampus during successful memory formation. Hippocampus, 15, 997–1005. [PubMed: 16281291]

Ranganath C, & Ritchey M (2012). Two cortical systems for memory-guided behaviour. Nature Reviews Neuroscience, 13, 713–726. [PubMed: 22992647]

Raz N, Lindenberger U, Rodrigue KM, Kennedy KM, Head D, Williamson A, et al. (2005). Regional brain changes in aging healthy adults: General trends, individual differences and modifiers. Cerebral Cortex, 15, 1676–1689. [PubMed: 15703252]

Ritchey M, Libby LA, & Ranganath C (2015). Corticohippocampal systems involved in memory and cognition: The PMAT framework. Connected Hippocampus, 219, 45–64.

Romano A, Guo J, Prokscha T, Meyer T, Hirsch S, Braun J, et al. (2014). In vivo waveguide elastography: Effects of neurodegeneration in patients with amyotrophic lateral sclerosis. Magnetic Resonance Medicine, 72, 1755–1761.

Rose M, Haider H, Weiller C, & Buchel C (2002). The role of medial temporal lobe structures in implicit learning: An event-related fMRI study. Neuron, 36, 1221–1231. [PubMed: 12495634]

Rubin RD, Schwarb H, Lucas HD, Dulas MR, & Cohen NJ (2017). Dynamic hippocampal and prefrontal contributions to memory processes and representations blur the boundaries of traditional cognitive domains. Brain Sciences, 7, E82. [PubMed: 28704928]

Rubin RD, Watson PD, Duff MC, & Cohen NJ (2014). The role of the hippocampus in flexible cognition and social behavior. Frontiers in Human Neuroscience, 8, 742. [PubMed: 25324753]

Rudebeck SR, Scholz J, Millington R, Rohenkohl G, Johansen-Berg H, & Lee AC (2009). Fornix microstructure correlates with recollection but not familiarity memory. Journal of Neuroscience, 29, 14987–14992. [PubMed: 19940194]

Ryan JD, Althoff RR, Whitlow S, & Cohen NJ (2000).Amnesia is a deficit in relational memory. Psychological Science, 11, 454–461. [PubMed: 11202489]

Sack I, Beierbach B, Wuerfel J, Klatt D, Hamhaber U,Papazoglou S, et al. (2009). The impact of aging and gender on brain viscoelasticity. Neuroimage, 46, 652–657. [PubMed: 19281851]

Sack I, Johrens K, Wurfel J, & Braun J (2013). Structure-sensitive elastography: On the viscoelastic powerlaw behavior of in vivo human tissue in health and disease. Soft Matter, 9, 5672–5680.

Sack I, Streitberger KJ, Krefting D, Paul F, & Braun J(2011). The influence of physiological aging and atrophy on brain viscoelastic properties in humans. PLoS One, 6, e23451. [PubMed: 21931599]

Sandroff BM, Johnson CL, & Motl RW (2017). Exercise training effects on memory and hippocampal viscoelasticity in multiple sclerosis: A novel application of magnetic resonance elastography. Neuroradiology, 59, 61–67. [PubMed: 27889837]

Sasson E, Doniger GM, Pasternak O, Tarrasch R, & Assaf Y (2013). White matter correlates of cognitive domains in normal aging with diffusion tensor imaging. Frontiers in Neuroscience, 7, 32. [PubMed: 23493587]

Schendan HE, Searl MM, Melrose RJ, & Stern CE(2003). An fMRI study of the role of the medial temporal lobe in implicit and explicit sequence learning. Neuron, 37, 1013–1025. [PubMed: 12670429]

Schlichting ML, Mumford JA, & Preston AR (2015). Learning-related representational changes reveal dissociable integration and separation signatures in the hippocampus and prefrontal cortex. Nature Communications, 6, 8151.

Schlichting ML, & Preston AR (2015). Memory integration: Neural mechanisms and implications for behavior. Current Opinion in Behavioral Sciences, 1, 1–8. [PubMed: 25750931]

Schregel K, Wuerfel E, Garteiser P, Gemeinhardt I, Prozorovski T, Aktas O, et al. (2012). Demyelination reduces brain parenchymal stiffness quantified in vivo by magnetic resonance elastography. Proceedings of the National Academy of Sciences, U.S.A., 109, 6650–6655.

Schwarb H, Johnson CL, Daugherty AM, Hillman CH, Kramer AF, Cohen NJ, et al. (2017). Aerobic fitness, hippocampal viscoelasticity, and relational memory performance. Neuroimage, 153, 179–188. [PubMed: 28366763]

Schwarb H, Johnson CL, McGarry MD, & Cohen NJ (2016). Medial temporal lobe viscoelasticity and relational memory performance. Neuroimage, 132, 534–541. [PubMed: 26931816]

Schwarb H, Watson PD, Campbell K, Shander CL, Monti JM, Cooke GE, et al. (2015). Competition and cooperation among relational memory represenations. PLoS One, 10, e0143832. [PubMed: 26619203]

Seger CA, & Cincotta CM (2006). Dynamics of frontal, striatal, and hippocampal systems during rule learning. Cerebral Cortex, 16, 1546–1555. [PubMed: 16373455]

Sexton CE, Mackay CE, Lonie JA, Bastin ME,Terrière E, O'Carroll RE, et al. (2010). MRI correlates of episodic memory in Alzheimer's disease, mild cognitive impairment, and healthy aging. Psychiatry Research, 184, 57–62. [PubMed: 20832251]

Simons JS, & Spiers HJ (2003). Prefrontal and medial temporal lobe interactions in long-term memory. Nature Reviews Neuroscience, 4, 637–648. [PubMed: 12894239]

Slotnick SD (2017). Cluster success: fMRI inferences for spatial extent have acceptable false-positive rates. Cognitive Neuroscience, 8, 150–155. [PubMed: 28403749]

Slotnick SD, Moo LR, Krauss G, & Hart J Jr. (2003). Distinct prefrontal cortex activity associated with item memory and source memory for visual shapes. Cognitive Brain Research, 17, 75–82. [PubMed: 12763194]

Smith SM, Jenkinson M, Johansen-Berg H, Rueckert D, Nichols TE, Mackay CE, et al. (2006). Tract-based spatial statistics: Voxelwise analysis of multi-subject diffusion data. Neuroimage, 31, 1487–1505. [PubMed: 16624579]

Smith C, & Squire LR (2005). Declarative memory, awareness, and transitive inference. Journal of Neuroscience, 25, 10138–10146. [PubMed: 16267221]

Spalding KN, Schlichting ML, Zeithamova D, Preston AR, Tranel D, Duff MC, et al. (2018). Ventromedial prefrontal cortex is necessary for normal associative inference and memory integration. Journal of Neuroscience, 38, 3767–3775. [PubMed: 29555854]

Spiers HJ, Maguire EA, & Burgess N (2001). Hippocampal amnesia. Neurocase, 7, 357–382. [PubMed: 11744778]

Steiger JH (1980). Tests for comparing elements of a correlation matrix. Psychological Bulletin, 87, 245–251.

Streitberger KJ, Sack I, Krefting D, Pfuller C, Braun J, Paul F, et al. (2012). Brain viscoelasticity alteration in chronic-progressive multiple sclerosis. PLoS One, 7, e29888. [PubMed: 22276134]

Tsivilis D, Vann SD, Denby C, Roberts N, Mayes AR, Montaldi D, et al. (2008). A disproportionate role for the fornix and mammillary bodies in recall versus recognition memory. Nature Neuroscience, 11, 834–842. [PubMed: 18552840]

Turner BO, Paul EJ, Miller MB, & Barbey AK (2018). Small sample sizes reduce the replicability of task-based fMRI studies. Communications Biology, 1, 62. [PubMed: 30271944]

Vilberg KL, & Rugg MD (2008). Memory retrieval and the parietal cortex: A review of evidence from a dual-process perspective. Neuropsychologia, 46, 1787–1799. [PubMed: 18343462]

Von Der Heide RJ, Skipper LM, Klobusicky E, & Olson IR (2013). Dissecting the uncinate fasciculus: Disorders, controversies and a hypothesis. Brain, 136, 1692–1707. [PubMed: 23649697]

Voss JL, Bridge DJ, Cohen NJ, & Walker JA (2017). A closer look at the hippocampus and memory. Trends in Cognitive Sciences, 21, 577–588. [PubMed: 28625353]

Voss JL, Warren DE, Gonsalves BD, Federmeier KD, Tranel D, & Cohen NJ (2011). Spontaneous revisitation during visual exploration as a link among strategic behavior, learning, and the hippocampus. Proceedings of the National Academy of Sciences, U.S.A, 108, E402–E409.

Wagner AD, Shannon BJ, Kahn I, & Buckner RL (2005). Parietal lobe contributions to episodic memory retrieval. Trends in Cognitive Sciences, 9, 445–453. [PubMed: 16054861]

Wang JX, Cohen NJ, & Voss JL (2015). Covert rapid action-memory simulation (CRAMS): A hypothesis of hippocampal-prefrontal interactions for adaptive behavior. Neurobiology of Learning and Memory, 117, 22–33. [PubMed: 24752152]

Wendelken C, Lee JK, Pospisil J, Sastre M III, Ross JM, Bunge SA, et al. (2015). White matter tracts connected to the medial temporal lobe support the development of mnemonic control. Cerebral Cortex, 25, 2574–2583. [PubMed: 24675870]

Worsley KJ, & Friston KJ (1995). Analysis of fMRI time-series revisited—Again. Neuroimage, 2, 173–181. [PubMed: 9343600]

Zalesak M, & Heckers S (2009). The role of the hippocampus in transitive inference. Psychiatry Research: Neuroimaging, 172, 24–30. [PubMed: 19216061]

Zeithamova D, Dominick AL, & Preston AR (2012).Hippocampal and ventral medial prefrontal activation during retrieval-mediated learning supports novel inference. Neuron, 75, 168–179. [PubMed: 22794270]

Zeithamova D, & Preston AR (2010). Flexible memories: Differential roles for medial temporal lobe and prefrontal cortex in cross-episode binding. Journal of Neuroscience, 30, 14676–14684. [PubMed: 21048124]

Zeithamova D, Schlichting ML, & Preston AR (2012). The hippocampus and inferential reasoning: Building memories to navigate future decisions. Frontiers in Human Neuroscience, 6, 70. [PubMed: 22470333]

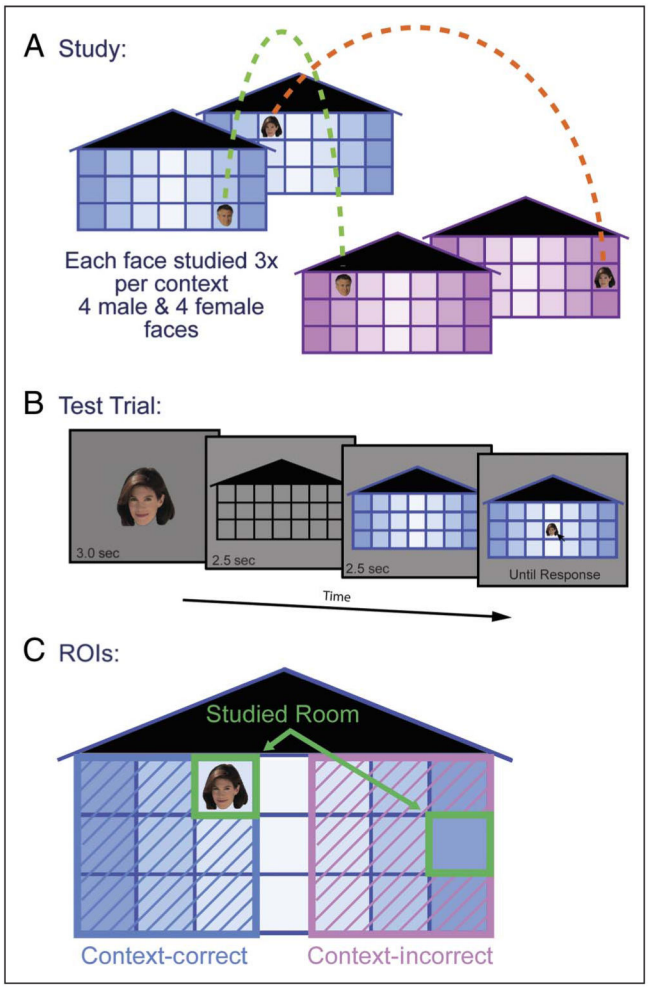

Figure 1.

Context-dependent relational memory task stimuli and design.(A) Study phase design. (B) Test phase design and timing information.(C) ROIs for behavioral responses. The four ROIs include the CC side of the building, the studied room on the context-correct (CC) side of the building (i.e., CC-studied room), the context-incorrect (CI) side of the building, and the studied room on the CI side of the building (i.e., CI-studied room).

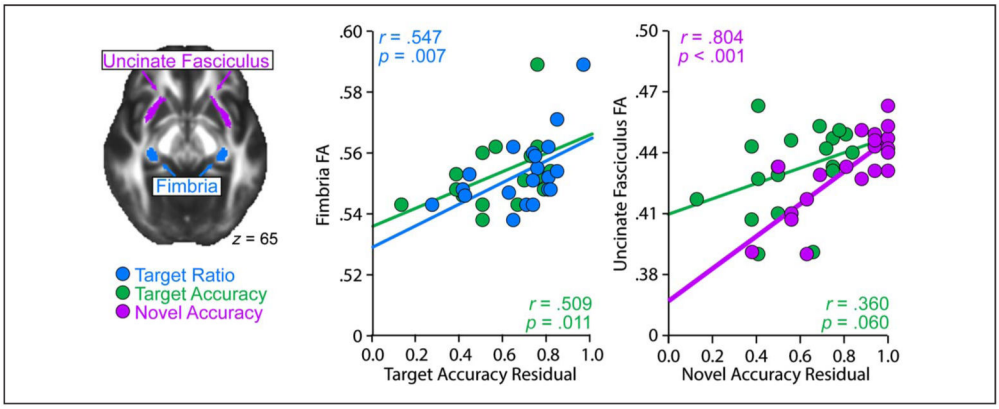

Figure 2.

DTI results. Fimbria FA significantly correlated with both Target Ratio and Target Accuracy, whereas UF FA significantly correlated with Novel Accuracy.

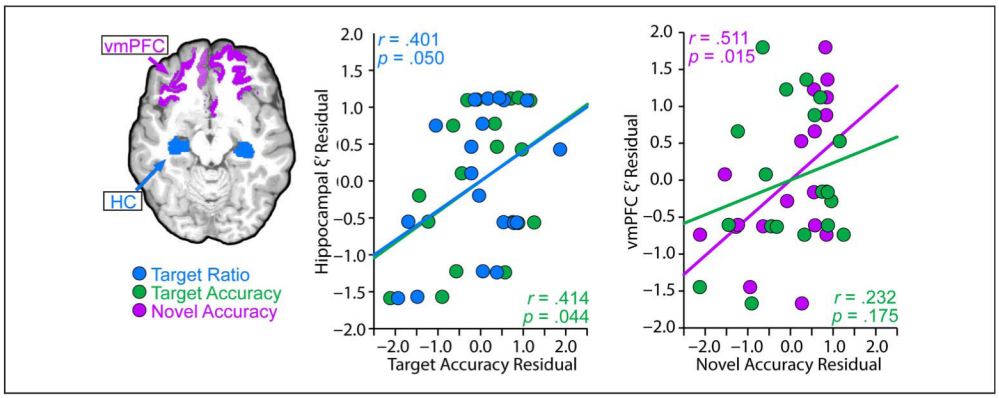

Figure 3.

MRE results. Hippocampal viscoelasticity (adjusted damping ratio, ξ') significantly correlated with target accuracy and the target ratio, whereas vmPFC/OFC viscoelasticity significantly correlated with novel accuracy. Behavioral and structural measure residuals, accounting for age, are plotted.

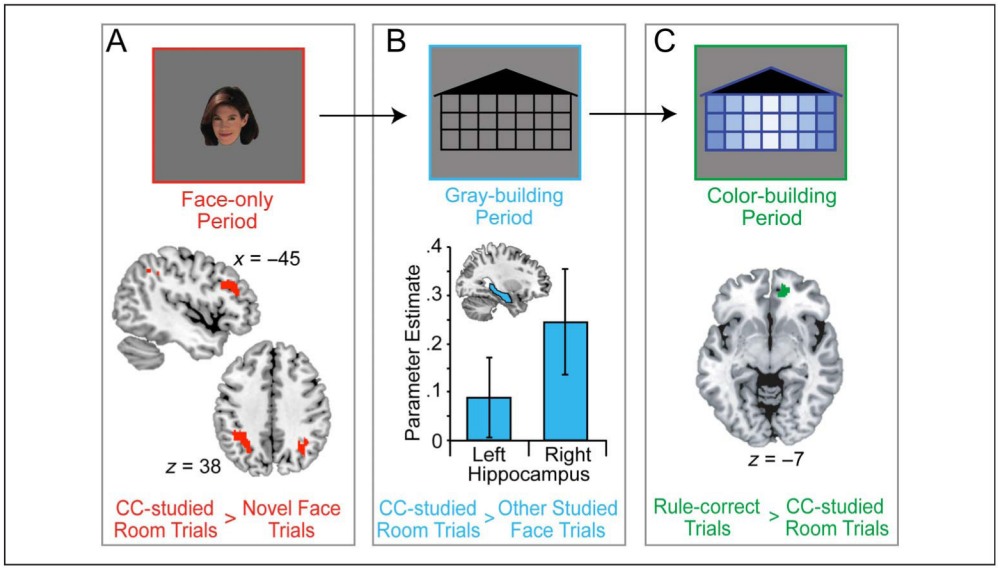

Figure 4.

fMRI results.(A) Activation maps comparing CC-studied room trials with novel face trials (old/new effect) during the face-only period.(B) Hippocampal ROI analysis comparing CC-studied room trials to all other studied face trials during the gray-building period. (C) Activation maps comparing trials where participants relied on rule information to CC-studied room trials during the color-building period.

Table 1.

Face-only Period Activation

Region	Coordinates	t Value	Voxels
Frontal			
Left inferior frontal gyrus, triangular	−45 35 23	4.10	58
Parietal			
Left inferior parietal/angular gyrus	−39 −43 38	5.42	115
Right inferior parietal/angular gyrus	33 −58 38	5.23	56

Table 2.

Color-building Period Activation

Region	Coordinates	t Value	Voxels
Frontal			
Right medial orbital frontal gyrus	15 50 −7	4.20	35